State-to-state reaction dynamics

Tunable lasers facilitate the finding of relative probabilities for forming product molecules in specified quantum states from reagents in selected states, a long-standing objective in chemical dynamics.

Richard N. Zare and Richard B. Bernstein

The study of chemical reaction kinetics can be likened to the task of making a motion picture of a reaction. The trouble thus far with achieving this goal seems to be the problem of too many would-be actors who strut upon the stage without proper cue and mumble their lines too rapidly to be understood—for chemical reactions occur with the ease of striking a match and at a speed so fast (on a subpicosecond time scale for the making of new bonds and breaking of old ones) as to be a severe challenge to the moviemaker who would like to record individual frames.

The laser (through its monochromaticity, tunability, and intensity) presents chemists with the opportunity of coming closer to the realization of this goal.[1] Lasers make possible the preparation of reagents in specific excited internal states, serving thereby as *effectors* of chemical change, and the identification and internal state analysis of the reaction products, used as *detectors* of chemical change. Yet a third usage of the laser is still in its infancy; it can provide radiation fields sufficient to influence intermolecular interactions during the subpicosecond interval in which the reagents are intimately interlocked. Nonresonant, laser-assisted collisional processes are then found to occur.

Most of our attention in this article will be devoted to the use of tunable lasers as effectors and detectors of chemical change. The hitherto inaccessible detailed information on molecular dynamics that they provide arises from the knowledge we gain of the internal states of reagents and products. A significant fraction of reagent molecules may be excited by resonant laser radiation to some desired internal state (electronic, vibrational, rotational) so that one can then measure the influence of the quantum state of the reagent upon its reactivity. When another tunable laser excites and probes the nascent product molecules in their various quantum states, the resulting laser-induced fluorescence and absorption can often reveal the internal state distribution of the products. Thus one can measure "state-to-state" (reagent-to-product) reaction rates and cross sections.[2]

The authors are professors in the chemistry departments of Stanford University (Zare) and Columbia University (Bernstein).

The problem

In the old days, kineticists had to be content with observing the overall rates of chemical reaction as a function of temperature. In the simplest such experiments, say, for the bimolecular gas phase reaction $A + BC \rightarrow AB + C$, one allows gaseous atoms A to come into contact with molecules BC and monitors the rate of removal of a reactant (A or BC) or the rate of appearance of a product (AB or C). Thus the rate R is given in terms of rates of change of the various number densities n as:

$$R = -\frac{dn_A}{dt} = -\frac{dn_{BC}}{dt} = +\frac{dn_{AB}}{dt} = +\frac{dn_c}{dt}$$

The initial rate of reaction depends upon the product of the reagent concentrations: $R = kn_A n_{BC}$, where k is the temperature-dependent rate coefficient. Note that $k(T)$ can be represented by the sum

$$k(T) = \sum_i F_i(T) k_i(T) \qquad (1)$$

where $F_i(T)$ is the fraction of reagents in some initial set of internal states i at the temperature T, and $k_i(T)$ is the total rate constant for all processes out of the set i into the final set of states f of the products:

$$k_i(T) = \sum_f k_{fi}(T) \qquad (2)$$

Before the turn of the century, Svante Arrhenius and others established the temperature dependence of the rate constant via careful observation. The empirical Arrhenius equation is

$$k(T) = A \exp(-E_a/kT) \qquad (3)$$

where the pre-exponential factor A depends only weakly on temperature; the constant E_a is called the activation energy. Since then, a large body of extremely useful data has been garnered on the individual values of A and E_a for various pairs of reactants, permitting chemists to model such complex phenomena as combustion in flames or the influence upon the stratospheric ozone layer of the release of chlorofluorocarbons into the atmosphere.

However, it was not until fairly recently that state-to-state rates could be measured.[2] Even these thermal rate constants $k_{fi}(T)$ are rather removed from the "picture" that chemists visualize of the process of combination between reactants and the separation of nascent products in the course of a reactive encounter.

Let us consider this matter in more detail. We can represent a reactive scattering event by means of the diagram shown as figure 1. By knowing the asymptotic states of the products, we wish to infer the details of the collision event. Given precisely defined initial and final states this is at least conceptually plausible. One could determine the state-to-state reaction cross sections $\sigma_{fi}(v_r)$, where v_r is the magnitude of the incident relative velocity ($v_r = \kappa\hbar/\mu$, where μ is the reduced mass of the reagent pair and κ the incident wave number), related to

0031-9228 / 80 / 110043-08 / $00.50

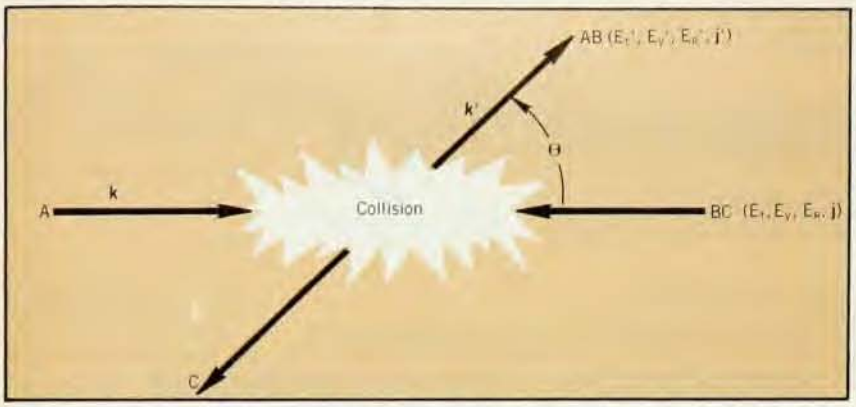

A "before and after" representation of an atom–diatom exchange reaction: The reactants A and BC in specified translational and internal states undergo collision to form the products AB and C. Here E_V, E_R, E_T are the vibrational, rotational and relative translational energies, **k** is a unit vector pointing along the relative velocity of the collision partners, and **j** is a unit vector along the rotational angular momentum of the molecules. Primed quantities refer to the products, unprimed quantities to the reagents. The angle $\theta \equiv$ arc cos (**k**·**k**') is the product scattering angle. Figure 1

the state-to-state rate coefficients by

$$k_{fi}(v_r) = v_r \sigma_{fi}(v_r) \qquad (4)$$

The state-to-state cross sections could be predicted from theory if the intermolecular forces, or the "potential energy hypersurface," were fully known.

Unfortunately, thermal initial conditions imply that the reagents' translational and internal state energy distributions are Maxwell–Boltzmann in nature, causing the nature of individual collision events to be "buried" inside averages over thermal distributions. This result is readily seen from the relation between the total rate constant $k(T)$ at a temperature T and the individual state-to-state cross sections $\sigma_{fi}(E_T)$ at a given relative translational energy E_T;

$$k(T) = (\pi\mu)^{-1/2}(2/kT)^{3/2} \sum_f \sum_i F_i(T) \times \int_0^\infty E_T \sigma_{fi}(E_T) \exp(-E_T/kT) dE_T \qquad (5)$$

From equation 5 it is apparent that the state-to-state cross sections $\sigma_{fi}(E_T)$ cannot be readily extracted from measurements of $k(T)$!

This conclusion may be restated in yet another way. Everyone knows that the rates of most chemical reactions are accelerated by heating. However, it is far from obvious in our reaction A + BC whether the increase in rate with temperature arises from the increased number of reagents that collide with enhanced translational energy or the increased number of reagent molecules with enhanced internal state energies. Which form of energization is more effective in promoting reaction? An answer to this question is unavailable from thermal kinetic studies because the translational and internal degrees of freedom of the reagents are in thermal equilibrium. Thus, one must devise nonequilibrium experiments in which the reagents' modes can be energized independently and the products' final states can be separately identified and monitored.

The molecular-beam scattering technique is well-suited for the measurement of reaction cross sections (especially angular distributions of the products of reactive scattering). The early experiments (by Sheldon Datz and Ellison H. Taylor, by Dudley R. Herschbach and his co-workers, and others) employed Maxwell–Boltzmann beams and thus provided only "averaged" information. Improvements such as reagent velocity selection and product velocity analysis, nozzle beam sources, and spectroscopic means of product state detection, have led to more refined cross-section data—usually however, on ground-state reagents as a function of relative translational energy. Recent molecular-beam experiments with better monochromaticity and higher energy resolution (by J. Peter Toennies and his co-workers, Yuan T. Lee and his group at Berkeley, Udo Buck and Hans Pauly, W. Ronald Gentry and Clayton F. Giese and their co-workers, and others) have, in special cases, yielded pure state-to-state inelastic and reactive cross sections, for near-ground-state reagents.

In what follows we review briefly the theoretical constructs used to describe state-to-state dynamics and then present some highlights of present research efforts.

Theoretical background

Low-energy collisions (both reactive and nonreactive) of heavy particles can usually be treated within the framework of the Born–Oppenheimer approximation. The nuclei may be regarded as moving under the action of a force field arising from a potential (due to the electrons) that depends only upon the nuclear configuration (distances and angles between nuclei). From this viewpoint reaction dynamics reduces "merely" to a computational problem. Given the potential energy function at all configurations en route from reactants to products, one solves for the motion of the nuclei on this energy hypersurface. Because for most systems of chemical interest the de Broglie wavelengths of the moving nuclei are small, classical mechanics (Hamilton's equations of motion) may be used to follow the gross motion of the nuclei during the "trajectory" of a reactive (or nonreactive) encounter, as shown nearly half a century ago by Henry Eyring and Joseph O. Hirschfelder. Of course, in this procedure averages must be taken over all initial conditions not specified experimentally, such as orientations, impact parameters, phases of the vibrational and rotational motions, and so on.

One of the significant recent trends in applied quantum chemistry is the development of computationally tractable schemes for the evaluation of "chemically accurate" potential surfaces, that is, beyond the London–Eyring–Polanyi–Sato (LEPS) level. Such calculations necessarily include electron correlation—they go beyond the variational optimization of a single electron configuration. As a consequence, very few surfaces are known with sufficient accuracy to obtain reliable chemical-dynamics predictions, and the major thrust of most activity in this field is experimentally directed. Nevertheless, we should not forget that the goal of these studies is to relate the dynamical features of a chemical reaction to the topology of a potential energy surface that mediates between reactants and products.

For an N-atom system, the potential function V depends on $3N-6$ coordinates, the internal degrees of freedom. To aid in visualizing the form of V, it is customary to constrain (freeze) some of these coordinates. Consider for example the three-atom system, ABC, appropriate to the A + BC reaction. For a *fixed* ABC bond angle, there are only two independent internuclear separations, say r_{AB} and r_{BC}. The dependence of V on these "bond lengths" can be represented as a surface, which can be visualized by a contour map.

Figure 2 shows two such slices through the three-dimensional potential function, one for a linear, the other for a bent configuration. The contours represent lines of constant energy, resembling the contours on a topographical map (lines of constant elevation). Where the contours crowd together, the gradient is steep, and where they spread apart the potential is nearly

flat. There are two valleys, the one at the lower right corresponding to the A + BC reactants and one at the upper left corresponding to the AB + C products. The "profile" of the lower right valley, at very large r_{AB}, is the potential energy curve for the diatomic reagent molecule BC, and similarly for the upper valley, referring to AB. The zero of energy is referenced to the reagents at infinite separation. The reaction is exoergic, releasing energy in going from reactants to products. We can trace out a "trajectory" of a colliding pair of reagents by plotting the calculated locus of points (r_{AB}, r_{BC}) characterizing the ABC system starting from the initial conditions (lower right) to the final conditions (out of the upper left valley).

Despite the overall energy release for this chemical transformation, some energy is usually required to cross over from the reactant to the product valleys, because the floors of each valley slope upward, meeting in a "mountain pass" or saddle point region. In figure 2 the location of the pass is in the entrance valley, but for another system it could equally as well have occurred in the exit valley.

The preferred course of the chemical reaction can be thought of in the same terms as planning a hiking expedition with the aid of these contour maps, a journey requiring the least expenditure of energy. This preferred reaction path essentially follows the line of minimal energy from reactants to products.

From figures 2a and 2b we see that collinear approach to the BC bond is energetically more favorable than sideways approach. Nevertheless, in each case, the reaction path first climbs from the bottom of the entrance valley, reaches the mountain pass, and then "turns a corner" as it descends toward the bottom of the exit valley. A profile of the energy along the reaction path shows that the barrier to reaction is but a small fraction of the energy needed to rupture the reagent (BC) bond. Indeed, it is the existence of such low-energy passes between reactants and products that allows concerted chemical transformations to be so common.

Actually, none of the classically calculated reactive trajectories follows the minimum energy path, although a number will come close. Those reactants with insufficient energy to surmount the barrier or those with sufficient energy but with misdirected initial conditions are "reflected" by the barrier and return along the same valley that they entered. Such nonreactive collisions constitute inelastic and elastic scattering events. Note that equation 5 shows that thermal rate constants are averages over all energy and initial conditions. Roughly speaking then, the activation energy, E_a, corresponds to the energy required by the reagents to cross the reaction barrier, and the pre-exponential factor, A, is related to the probability that the colliding pairs of reagents have the "correct" initial conditions for reaction.

By following classical trajectories on a number of potential energy surfaces, a broad set of generalizations has emerged (largely from the work of John C. Polanyi and his co-workers, and the late Don L. Bunker) concerning the effect of specific features of the potential energy surface on the reaction dynamics across the surface. For potential surfaces that have deep minima or "potential wells," corresponding to stable ABC molecules, the reactants often become trapped for such a long time (many picoseconds) that the products carry away no memory of the nature of the reactants other than that imposed by the conservation of total energy and total angular momentum. For such "long-lived complexes" statistical behavior is often manifested. For other potentials in which the hollows are inaccessible or nonexistent, a direct-mode reaction occurs in which the interchange of collision partners happens "on the fly," in a time comparable to the period of a molecular vibration (around 10^{-13} sec). As the relative velocity of the reactants is increased, there is often a transition from the complex mode to the direct mode of reaction.

For direct reactions, the extent of product rotation reflects the preferred geometry as the mountain pass is crossed. A bent configuration will obviously lead to higher product rotational excitation than a collinear one. The

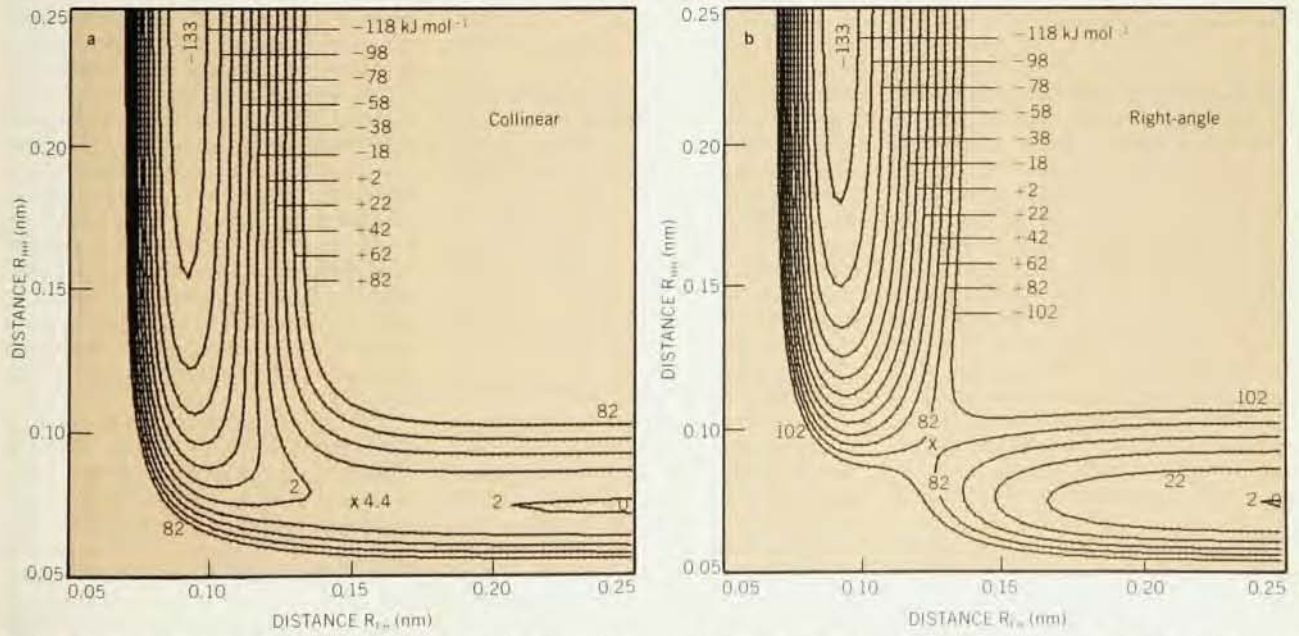

Contour plots of realistic potential energy surfaces for an A + BC reaction. Part **a** shows surface "M5" for the collinear reaction $F + H_2 \rightarrow HF + H$. R_{FH} is the distance between the F atom and the nearer H atom. Contours are spaced at 20kJ mol^{-1} intervals. The zero of potential energy is the "floor" of the reactant valley (lower right). A small barrier (x) of height 4.4_5 kJ mol^{-1} is in the entrance valley at $R_{FH} = 0.154$ nm, $R_{HH} = 0.076$ nm. Part **b** is for the same system, but here the FHH angle is constrained to 90°. The barrier to reaction is about 85 kJ mol^{-1}, substantially larger than that for the collinear reaction. (Adapted from J. T. Muckerman, Chapter 1 in *Theory of scattering: Papers Dedicated to Henry Eyring*, D. Henderson, ed., Academic, N.Y., 1980.) Figure 2

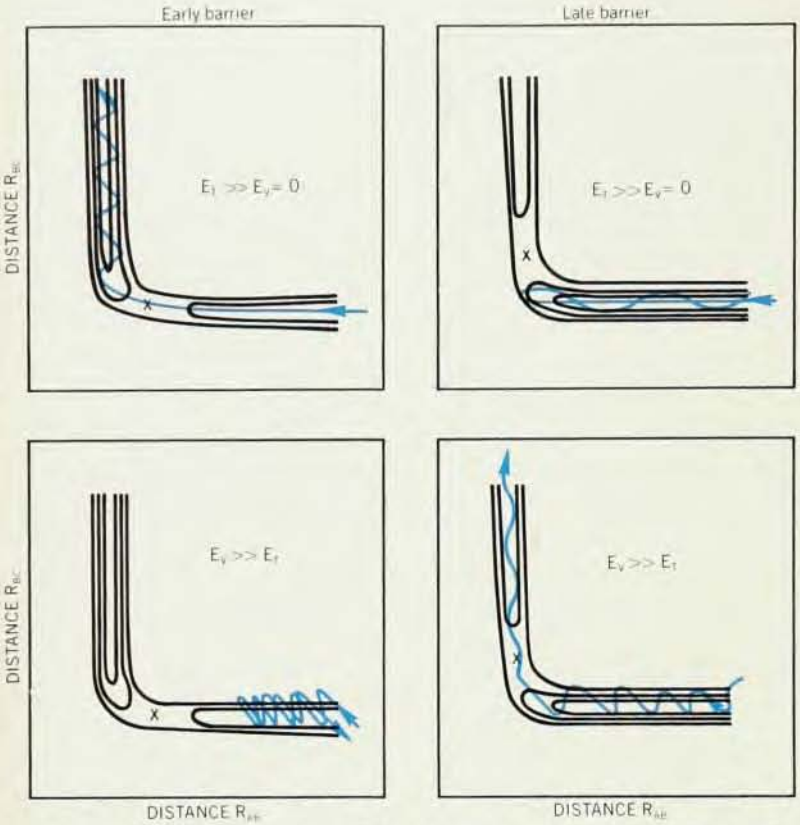

Classical trajectories on stylized potential-energy surfaces for the collinear A + B-C→AB + C reaction showing role of reagent's vibrational energy (E_V) and relative translational energy (E_T) in surmounting the activation barrier (x). In all cases the total energy exceeds the barrier height; so reaction is allowed on energetic grounds. When E_T is large (top row), reaction occurs for "early barrier" case but not for "late barrier." When E_V is large and E_T small (bottom row), reaction fails for early barrier, occurs for late barrier. Thus vibrational energy helps in surmounting a late barrier. (Adapted from J. C. Polanyi and W. H. Wong, J. Chem. Phys. **51**, 1439, 1969, and reference 1.) Figure 3

extent of product vibrational excitation is largely governed by the location of the barrier in the potential surface. If the barrier occurs "early" along the reaction path in the entrance valley, the energy released on crossing this barrier will be largely channeled into motion perpendicular to the exit valley direction, causing the AB product to oscillate between the walls of the exit valley. On the other hand, if the barrier occurs "late" in the reaction path, that is, *after* the reactants have skillfully turned the corner, then the energy release tends to go into relative translational motion of the products rather than vibrational excitation (see figure 3).

This discussion has stressed those factors influencing the disposal of the exoergicity of a reaction into product translation, vibration and rotation. However, by application of microscopic reversibility we can see that for the inverse, endoergic reaction certain forms of reagent excitation will be preferable to others in promoting reactivity. For example, reagent vibrational excitation is selective in enhancing the reaction rate if the barrier occurs late, while translational excitation favors overcoming early barriers located in the entrance channel. Although highly simplified, these models play an important role in interpreting state-to-state dynamics. Conversely, they also show how experimentally-derived dynamical information bears on the nature of the potential energy surface.

The "laser revolution in chemistry"

The field of molecular photochemistry has been an active one for more than half a century. Powerful lamps of various kinds have been used as sources of radiation in the ultraviolet and visible regions to initiate (and to monitor) chemical reactions. Then what is the basis of the claim implicit in the often-heard phrase "the laser revolution in chemistry"?[3] What's *really new* about laser-induced chemistry? It is the combination of intensity, monochromaticity, polarization, coherence, collimation, variable duration of pulse length, and tunability of laser light sources now available in the infrared, visible, and ultraviolet, which now makes possible both the *preparation* of chemically reactive molecules with unprecedented selectivity and the *detection* of products with extraordinary sensitivity.

Most laser studies of reaction dynamics fall into two broad categories: those that determine the specificity of formation of the various reaction products in different energy states, and those that determine the selectivity of the energy requirement in causing reaction to proceed.[4] Experimentalists are beginning to take advantage of the power of laser techniques by simultaneously controlling reagent states and probing product state distributions. In some very recent work strong laser fields have been used to influence chemical reactivity by exciting the reagent pair "collectively," during their encounter. In what follows we present a sampling of recent work to illustrate the growing use of lasers in investigating state-to-state chemical reaction dynamics.

The hydrogen exchange reaction

The "simplest" example of all neutral chemistry is the exchange reaction between a hydrogen atom and a hydrogen molecule

$$H + H_2 \rightarrow H_2 + H$$

and its isotopic analogues. Not surprisingly, the most accurately known potential energy surface for any reaction is that of the $H + H_2$ system. As shown in figure 4, this "atom exchange" reaction has an energy barrier; the threshold energy for reaction is about 32 kJ mol^{-1}. However, a single quantum of vibrational excitation in H_2 (50 kJ mol^{-1}) clearly exceeds that energy threshold. Thus this reaction is a good choice for assessing the effect of vibrational excitation on the reaction dynamics. Only recently have direct experimental investigations been possible, owing to the difficulty of preparing known concentrations of $H_2(v = 1)$. (Since H_2 is a nonpolar, infrared-inactive molecule, direct laser photoexcitation is not possible.)

A study of this system was recently reported by Michael Kneba, U. Wellhausen and Jürgen Wolfrum,[5] who measured the rate of the $D + H_2(v = 1)$ exchange reaction in a so-called "discharge flow" system. A low-pressure flow of HF and H_2 in a helium carrier gas was exposed to short pulses (10 microsec) from an HF laser tuned to the fundamental transition, $HF(v = 0 \rightarrow 1)$. Rapid population of $H_2(v = 1)$ occurs via near-resonant vibrational (V→V) transfer from $HF(v = 1)$. Deuterium atoms, generated by dissociation of D_2 in a microwave discharge, were intro-

duced upstream. The absolute concentrations of vibrationally excited HF molecules were determined from time-resolved infrared emission; the concentration of hydrogen atoms formed in the exchange reaction were determined from time-resolved absorption using Lyman-alpha resonance radiation. Because $H_2(v=0)$ molecules react relatively slowly with D atoms at room temperature, the concentrations of H_2 and D could be adjusted so that the formation of H atoms from the $D + H_2(v=0)$ exchange reaction gave no strong background absorption of the Lyman-alpha radiation without laser excitation. Moreover, the concentrations of H_2 and HF were chosen so that only a small fraction of the H_2 molecules was excited to $v=1$, ensuring that the concentration of $H_2(v>1)$ is essentially negligible.

Kneba, Wellhausen and Wolfrum[5] report a value for the bimolecular rate coefficient k for HD production at 298 K of around 10^{-11} cm^3 sec^{-1}, which is some 4×10^4 times faster than the thermal $H_2(v=0)$ rate constant! As yet there are no accurate quantum calculations of this rate. However, the latest quasi-classical trajectory calculations (employing an accurate H_3 potential energy surface) yield a rate at the same temperature that is smaller than this experimental result by a factor of about 40. It is not clear why this "simplest of all chemical processes" is not yet better understood. For a recent review of bimolecular reactions of vibrationally excited molecules, see reference 6.

Vibrational excitation

The use of infrared lasers generally limits vibrational excitation of reagents to $v=1$ (the fundamental), but it is possible to prepare reagents in higher states of vibrational excitation by direct laser pumping of a vibrational overtone, using visible wavelengths. This technique has been exploited by K. V. Reddy and Michael J. Berry,[7] who investigated the isomerization of state-selected allyl isocyanide, which proceeds according to the following kinetic mechanism:

$$H_2C{=}C(H)CH_2NC + h\nu \rightarrow H_2C{=}C(H)CH_2NC^{\dagger}$$

Photoactivation via C – H overtone absorptions

$$H_2C{=}C(H)CH_2NC^{\dagger} + M \rightarrow H_2C{=}C(H)CH_2NC$$

Collisional quenching

$$H_2C{=}C(H)CH_2NC^{\dagger} \rightarrow H_2C{=}C(H)CH_2CN$$

Isomerization (RCNC→RCCN)

Because the overtone absorption strength is so much weaker than the fundamental, the allyl isocyanide sample is placed *inside* the cavity of a dye laser tuned to the overtone of some specific CH stretching vibration. In allyl isocyanide there are three types of CH stretches: terminal olefinic ($H_2C=$), nonterminal olefinic ($=CH-$), and methylenic ($-CH_2-$). The rate constant for photoisomerization was measured as a function of pressure for each wavelength. The assumption was made that each collision of excited allyl isocyanide with the ambient gas molecules caused quenching, regardless of state of excitation; then the pressure of the bath gas serves as an internal clock for timing the rate of isomerization. Figure 5 compares the experimentally determined rate constants with those calculated from a statistical model (RRKM theory), which assumed that all energy is randomized among the internal degrees of freedom of the parent molecule prior to isomerization. There appear to be small but significant deviations from statistical behavior, suggesting that the isomerization rate of allyl isocyanide depends not only on its overall energy but also on the particular vibrational motion excited.

Experiments on vibrational excitation of molecules in the bulk gas phase suffer from the fact that collisions rapidly relax the initially selected rotational state or orientation of the reagent, although there is usually some persistence of the vibrational disequilibrium due to slow V→T collision rates. This restriction (collisional relaxation) is removed by carrying out laser excitation of free molecules in beams. This was first shown to be possible in 1971 by Philip R. Brooks and his co-workers who studied the reaction:

$$K + HCl(v=1) \rightarrow KCl + H$$

The excited hydrogen-chloride molecules are produced by resonant excitation via irradiation from a hydrogen-chloride chemical laser. The ground-state reaction is essentially thermoneutral; the reaction with $HCl(v=1)$ was found to be accelerated by about two orders of magnitude compared to $HCl(v=0)$. Recently H. H. Dispert, M. W. Geis and Brooks[8] succeeded in measuring relative reaction rates as a function of the rotational state J of the $v=1$ HCl molecules by using a grating-tuned HCl chemical laser for irradiation of the HCl beam. They found that the reactivity decreases significantly as the rotational angular momentum is increased by each unit of $\hbar$, for $J=1$ to $J=4$. This rotational inhibition of the $K + HCl(v=1, J)$ reaction must be a dynamical effect. Purely kinematic effects cannot be responsible for this behavior because most of the angular momentum of the reacting system is brought in as orbital angular momentum ($\sim 20\ \hbar$) of the collisional partners. Moreover, the energy change in going from J to $J+1$ is small compared to the relevant vibrational or translational energies. The possibility has been suggested that the origin of this rotational inhibition may stem from the need for preferential orientation of the reagents prior to reaction. For molecules rotating more rapidly, there is less time for the collision partners to spend in the spatial conformation that promotes reaction.

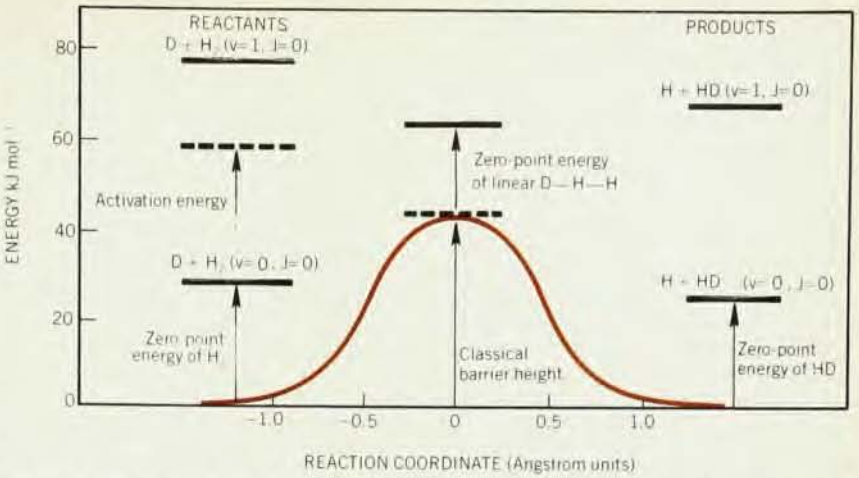

Potential-energy diagram for the reaction $D + H_2$ ($v=0,1$). The reactants are assumed to approach in a "collinear" orientation. (Adapted from reference 5). Figure 4

Molecular orientation

Laser excitation may also be used to determine the dependence of the reaction cross section upon the molecular orientation (for an atom–molecule reaction). Ziv Karny, Ronald C. Estler and Zare[9] have studied the reaction:

$$Sr + HF(v=1, J) \rightarrow SrF + H$$

under single-collision conditions in which a beam of strontium atoms traverses a scattering cell filled with HF

from a pulsed chemical HF laser interacts with the HF molecules, it preferentially excites those molecules whose dipole moments are collinear with the electric vector of the light beam; the probability of excitation varies as $\cos^2\theta$, where θ is the angle between the HF internuclear axis and the electric vector. Even though the HF molecule may rotate many times before making a collision with strontium atom, a memory of the preferred orientation still persists because the optical pumping process selects the total angular momentum vector, **J**, of the HF molecule, and the direction of **J** is preserved (in the absence of external fields) until collision occurs. Karny, Estler and Zare[9] found marked differences as a function of HF($v = 1$) orientation.

The orientation-dependence of the reactivity of ground-state molecules had been observed fifteen years ago (by Brooks and co-workers and by Robert J. Beuhler and Bernstein) using the difficult technique of state selection, electrostatic focusing and orientation by an electric field. The new laser technique, which employs polarized beams of (excited) reagent molecules, should open up the possibility of detailed study (for many new systems) of the steric factors that control reactivity.

Laser-induced fluorescence

The laser is also serving as a key tool in product state analysis, chiefly through the technique of laser-induced fluorescence.[10] Light from a tunable laser is directed into the reaction zone to be probed. As the wavelength of the laser is scanned, molecules within the reaction zone will be excited when the laser output overlaps an absorption line. Once excited, the molecules may fluoresce—that is, they re-emit radiation; some fraction of the fluorescence is detected by a photomultiplier. By recording the photomultiplier output as a function of laser wavelength one obtains a so-called "excitation spectrum." By using pulsed lasers and delaying the detection gate one can easily avoid the interference from scattered laser light. The observation of bright fluorescence against a dark background makes the laser-induced fluorescence technique extremely sensitive; molecular densities in the range of 10^4–10^5 cm^{-3} have been successfully detected without the use of extensive signal averaging.

Not all molecules are suitable candidates for detection by this technique since they do not all fluoresce with high efficiency, or have spectroscopically analysed fluorescence bands, or have fluorescence bands easily accessed by currently available tunable lasers. Moreover, the determination of relative quantum state populations from

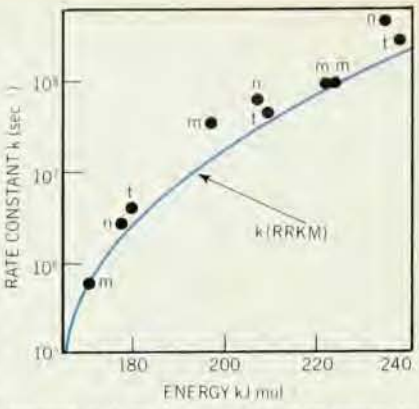

Unimolecular isomerization of allyl isocyanide. The rate constant $K(\epsilon)$ was measured after laser excitation via $5\nu_{CH}$ ($170 < \epsilon < 180$ kJ mol^{-1}), $6\nu_{CH}$ ($197 < \epsilon < 210$) and $7\nu_{CH}$ ($223 < \epsilon < 239$). Symbols t, n and m indicate terminal, nonterminal and methylenic CH stretch. The curved line is a calculation via RRKM theory. (From reference 7.) Figure 5

the measured intensities of the spectral features requires accurate vibrational band strengths (Franck–Condon factors) and rotational line strengths (Hönl–London factors). Lack of this knowledge reduces the pool of possible candidates for analysis by laser-induced fluorescence. However, when the technique *can* be employed, it brings all the power and richness of molecular spectroscopy to bear on the internal state analysis of nascent reaction products.[10]

Figure 6 shows an example of the use of the laser-induced fluorescence taken from the work of Charles M. Miller and Zare.[11] A molecular beam of vinyl cyanide, $H_2C{=}CH(CN)$, is irradiated by the pulsed output of a high-power CO_2 laser, which causes infrared multiphoton dissociation of the parent compound. (For a full discussion of this technique see the companion article by Yuan Lee and Ron Shen on page 52.) The CN radical has an electronic band system around 385 nm. An analysis of the intensity pattern of the individual lines leads to the conclusion that the unrelaxed CN fragment is born with a rotational distribution well characterized by a Boltzmann temperature. This result further supports the picture that the excitation energy is statistically redistributed in the multiphoton dissociation process.

The dissociative dynamics of molecules is a matter of much fascination, because the process can be viewed as a "half collision" of the recoiling fragments. An intriguing study of the photodissociation of hydrogen peroxide, H_2O_2, is underway at Columbia University by Richard Bersohn, Gerald Ondrey, Sheldon Kanfer and M. Kawasaki, who have irradiated H_2O_2 molecules by the 193 nm photons of an ArF laser and detected the OH radicals by laser-induced fluorescence, using a flashlamp-pumped tunable dye laser (Rh6G). Although an energy of more than 4 eV is deposited in a molecule of H_2O_2 in excess of that required to form two ground-state OH fragments, no vibrationally hot OH molecules were detected. Moreover, even though the rotational distribution extends as far out as $K'' = 20$, the lowest rotational levels are the most highly populated. The ground-state geometry of HOOH is known to be a bent structure in which the two HOO planes are nearly perpendicular to one another. The geometry of the dissociative excited state is unknown. These results suggest that the energy release is directed essentially along the O-O bond, thus exerting little torque on the departing OH fragments, since the center of mass of the OH molecule almost coincides with the O nucleus. We do not yet know if both OH fragments are in the ground electronic state or if one is electronically excited.

The OH radical, like CN, is particularly well-suited for laser-induced fluorescence studies because its spectrum has such an "open" structure, allowing easy resolution of individual features. Recently, this property has been exploited by Peter Andresen and Alan C. Luntz[12] who carried out a series of crossed-beam reactions of oxygen atoms with various alkanes. For these single-collision combustion processes, Andreson and Luntz used laser-induced fluorescence to determine the nascent internal state distribution of the OH product for a variety of different saturated hydrocarbons, corresponding to abstraction of primary (H—C—), secondary (H—C—H) and tertiary (H—C—) hydrogen atoms.

In all cases the OH rotational distributions are nearly identical, peaking at the lowest rotational level. This suggests that these reactions favor collinear attack of the O(^{3}P) atom to the H-C bond. However, the vibrational state distribution of OH depends markedly on the type of hydrogen atom abstracted, the degree of vibrational excitation increasing significantly in going from primary to secondary to tertiary. This behavior is interpreted as a shift in the nature of the potential energy hypersurface from repulsive to attractive across this series; in other words, the critical region where the C-H bond "breaks" moves from the exit toward the entrance valley.

In addition, the fine-structure levels are unequally populated. Spin–orbit interaction in the rotating $^2\Pi$ radical causes a vibrational–rotational level to be split by about 125 cm^{-1} into two spin

doublets, each of which is further split into two Λ doublets separated by less than 1 cm^{-1}. These four fine structure substrates of each (v,K) level can be individually probed by laser-induced fluorescence. While no preference for different Λ doublets was detected, Andreson and Luntz observed the spin components to be populated selectively.[12] In the adiabatic limit, $O(^3P_2)$ correlates with $OH(^2\Pi_{3/2})$ through a $^3\Pi_2$ reaction surface, $O(^3P_0)$ connects to $OH(^2\Pi_{1/2})$ through a $^3\Pi_0$ surface, while $O(^3P_1)$ does not correlate with $OH(^2\Pi_{1/2,3/2})$ at all. On the other hand, in the diabatic limit the population of the $^2\Pi_{1/2,3/2}$ spin doublets would be statistical. In Andreson and Luntz's experiment, most of the oxygen atoms were in the $^3P_2$ level. They found the ratio of the spin doublet populations to be about midway between the adiabatic and diabatic limits, implying that transitions between the $^3\Pi_2$ and $^3\Pi_0$ surfaces indeed occur to a significant extent during the course of a reactive encounter.

In all these studies the general picture emerges that the reactions of oxygen atoms with alkanes is dominated by interactions of $O(^3P)$ with the individual C-H bonds. This interpretation suggests that the rest of the molecule can be treated as a structureless particle, thus greatly simplifying the description of the dynamics of these reactions, which have obvious technological importance.

The laser-induced-fluorescence spectrum in the work described above is obtained by scanning the laser wavelength over different absorption lines. However, this type of measurement uses only part of the information available from this spectroscopic technique. Measurement of the Doppler profile of a single rotational line allows the recoil velocity distribution along the line of sight to be obtained for the product in a specific internal state; measurement of the Doppler profile at different scattering angles allows the full three-dimensional velocity distribution to be recovered. This concept, known as Fourier transform Doppler spectroscopy, was introduced in 1977 by James L. Kinsey.[13] The first successful application of the technique, carried out by him and his coworkers,[14] was a study of the exothermic reaction $H + NO_2 \rightarrow OH + NO$. They measured Doppler profiles at 20° intervals over a 180° angular range for the $R_1(17)$ line of the (0,0) band of the OH $A^2\Sigma^+ - X^2\Pi$ transition. The velocity-angle contours of the OH product flux show peaking along the H atom relative velocity vector (the so-called forward direction). This implies incomplete randomization of energy during the reactive collision. (This conclusion is also supported by the observation, by laser-induced fluorescence, of nonstatistical internal state distributions of the OH product.)

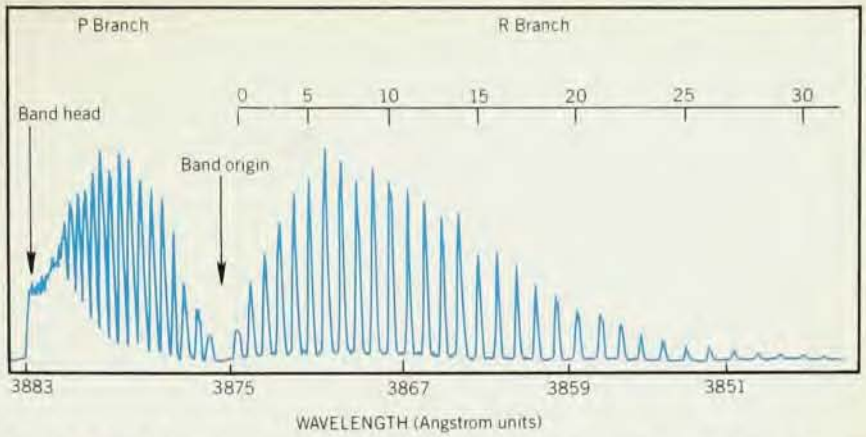

Laser-induced fluorescence excitation spectrum of CN, produced by the ir multiphoton dissociation of vinyl cyanide in a molecular beam, shows rotational structure of the (0 – 0) band of the $B^2\Sigma^+ - X^2\Sigma^+$ violet system. Relative populations of these levels are well-described by a rotational temperature of 453 ± 5 K. (Adapted from reference 11.) Figure 6

Multiphoton ionization

The sensitivity of laser-induced fluorescence detection can yet be improved upon by the method of laser multiphoton ionization, in which a molecule is ionized after absorbing more than one photon.[15] All charged fragments can be collected, mass-analyzed, and detected with nearly unit efficiency, which is not the case for fluorescent photons.[16] Moreover, in favorable cases, nearly every absorbing molecule can be ionized. Because the wavelength dependence of the multiphoton-ionization signal depends on the energy levels of the molecule under study, its spectrum can be used, in principle, to determine detailed internal state distributions. In practice the application of multiphoton ionization to product state analysis has been held back by the need to accumulate a body of information analogous to the spectroscopic data base that underlies laser-induced fluorescence. However, rapid progress is being made in understanding the photophysics of multiphoton ionization; the day is approaching when laser ionization mass spectrometry may become the method of choice, particularly for large molecules that do not fluoresce.

Recent work by Bernstein and his colleagues[17] illustrates the power of multiphoton ionization. They constructed a computer-controlled time-of-flight laser ionization mass spectrometer system. Its first application was to the molecule triethylenediamine, $N(C_2H_4)_3N$, ionized when a pulsed dye laser was scanned over two spectral regions, 520–562 nm and 420–440 nm. The former covers the two-photon $\tilde{A} \leftarrow \tilde{X}$ transition while the latter includes a band attributed to a two-photon transition to a component of the 3d-Rydberg state. As we show in figure 7, the ionization signal follows closely the absorption spectrum and the fragmentation pattern depends upon the excitation wavelength.

Thus multiphoton ionization gives to mass spectrometry the optical signature of the molecule. Although lacking the universality of electron impact ionization, multiphoton ionization has the ability to ionize each component in a mixture selectively. For example, David L. Lubman, Ron Naaman and Zare[18] recently reported the wavelength-selective detection of the two $C_{10}H_8$ isomers, azulene and naphthalene. Much work still needs to be done, however, both experimental and theoretical, before multiphoton ionization can be applied routinely to the analysis of reaction products.

Of course lasers can be used simultaneously to prepare reagents and probe products, and such experiments are just beginning.[19,20] An example is the reaction $Sr + HF(v = 1) \rightarrow SrF + H$ investigated by Arunava Gupta, David S. Perry and Zare.[19] They fired a beam of strontium atoms through a scattering chamber filled with HF gas at a pressure of 10^{-4}–10^{-5} torr. The ground-state HF ($v = 0$) reaction has an energy threshold of 27 ± 7 kJ mol^{-1}. When the HF gas is irradiated by a grating-tuned pulsed HF laser, SrF products appear and are detected by their characteristic laser fluorescence excitation spectrum. The rate of the $Sr + HF(v = 1)$ reaction (exothermic by 21 kJ mol^{-1}) is found to be orders of magnitude more rapid than that of the endothermic ground-state HF reaction. This study not only determined the internal state distribution of the SrF products (that is, the relative state-to-state cross sections) but also com-

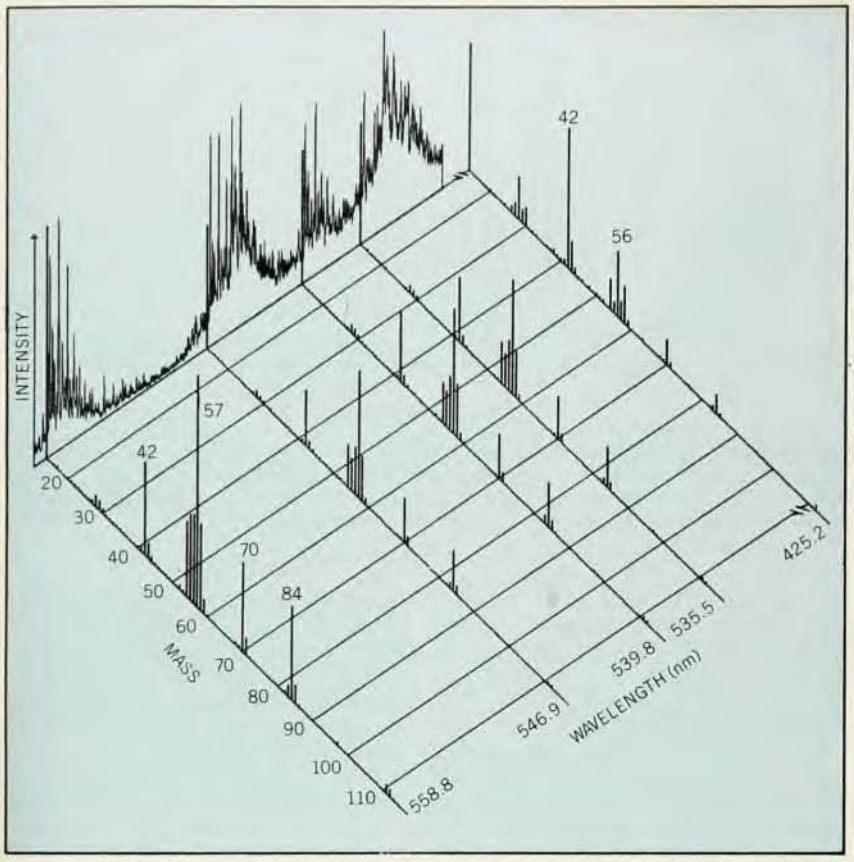

Two-dimensional vibronic/mass spectrum of triethylenediamine $[N(C_2H_4)_3N]$ obtained via laser multiphoton ionization mass spectroscopy. Back-panel: total ionization wavelength spectrum; sticks, relative intensities of fragment ions. (Adapted from reference 17.) Figure 7

pared the $Sr + HF(v = 1)$ reaction to the $Sr + HF(v = 0)$ reaction when the latter is carried out with excess collisional energy, in order to determine which form of energization is more effective in promoting reaction. Vibrational excitation is found to enhance the reaction rate from 1 to 10 times more than translational excitation at the same total energy. This result is in accord with the generalization mentioned earlier (see figure 2), namely, that barriers occurring late in the reaction path are more readily surmounted by reagent vibration.

Laser-assisted chemistry

We have been discussing examples in which lasers are used to prepare reagents, or probe products, or to do both simultaneously. However, there is also the third usage, hinted at earlier, which is still very much in its infancy. Lasers can provide radiation fields sufficient to influence intermolecular interactions during that brief moment that there are neither reagents nor products but a "transition state," thereby bringing about "laser-assisted chemistry."[21] Brooks and his coworkers[22] recently reported an application of this process to chemistry. They crossed a beam of potassium atoms with a molecular beam of mercury dibromide molecules and irradiated the interaction volume with the pulsed output of a flashlamp-pumped dye laser tuned to 595 nm. At this wavelength the laser can excite neither the reactants nor the products. When the laser is on, they observed weak luminescence at 500 nm, and they attributed it to emission from electronically excited mercury monobromide, $HgBr^*(B)$. This reaction product is postulated to be formed by light absorption by the collision complex, as follows:

$$K + BrHgBr \rightleftarrows [KBrHgBr]$$

complex formation

$$[KBrHgBr] + h\nu(595\ \text{nm}) \rightarrow KBr + HgBr^*(B)$$

photodecomposition

$$HgBr^*(B) \rightarrow HgBr(X) + h\nu(500\ \text{nm})$$

fluorescence

Such studies may permit one to probe the structure of "transition states" and to obtain direct information about the bond-making–bond-breaking process.

So we see in summary that, although an elementary chemical reaction can be viewed as an epic motion picture with a cast of countless characters, new laser techniques are enabling chemical physicists to dissect the many sub-plots involving the role of individual reactive collisions.

* * *

The authors' research programs in state-to-state dynamics are supported by grants from the National Science Foundation.

References

1. R. D. Levine, R. B. Bernstein, *Molecular Reaction Dynamics*, Clarendon Press, Oxford (1974).
2. P. R. Brooks, E. F. Hayes Jr, (eds.), *State-to-State Chemistry*, ACS Symposium Series No. 56, Amer. Chem. Soc., Wash. D.C. (1977).
3. J. I. Steinfeld, M. S. Wrighton, (eds.), *The Laser Revolution in Energy-Related Chemistry*, M.I.T. Press, Cambridge, Mass. (1976); T. F. George, (ed.), *Theoretical Aspects of Laser Radiation and its Interaction with Atomic and Molecular Systems*, Univ. of Rochester, N.Y. (1978).
4. R. D. Levine, R. B. Bernstein, Acc. Chem. Res. **7**, 393 (1974).
5. M. Kneba, U. Wellhausen, J. Wolfrum, Ber. Bunsenges. Phys. Chem. **83**, 940 (1979).
6. M. Kneba, J. Wolfrum, Ann. Rev. Phys. Chem. **31**, 47 (1980).
7. K. V. Reddy, M. J. Berry, Chem. Phys. Lett. **66**, 223 (1979).
8. H. H. Dispert, M. W. Geis, P. R. Brooks, J. Chem. Phys. **70**, 5317 (1979).
9. Z. Karny, R. C. Estler, R. N. Zare, J. Chem. Phys. **69**, 5199 (1978).
10. R. N. Zare, P. J. Dagdigian, Science **185**, 739 (1974); R. N. Zare, Far. Disc. Chem. Soc. **67**, 7 (1979); J. L. Kinsey, Ann. Rev. Phys. Chem. **28** 349 (1977).
11. C. M. Miller, R. N. Zare, Chem. Phys. Lett. **71**, 376 (1980).
12. P. Andresen, A. C. Luntz, J. Chem. Phys. **72**, 5842 (1980).
13. J. L. Kinsey, J. Chem. Phys. **66**, 2560 (1977).
14. E. J. Murphy, J. H. Brophy, G. S. Arnold, W. L. Dimpfl, J. L. Kinsey, J. Chem. Phys. **70**, 5910 (1979).
15. P. M. Johnson, Acc. Chem. Res. **13**, 20 (1980).
16. L. Zandee, R. B. Bernstein, J. Chem. Phys. **71**, 1359 (1979).
17. D. A. Lichtin, S. Datta-Ghosh, K. R. Newton, R. B. Bernstein, Chem. Phys. Lett. **75**, 214 (1980).
18. D. L. Lubman, R. Naaman, R. N. Zare, J. Chem. Phys. **72**, 3034 (1980).
19. A. Gupta, D. S. Perry, R. N. Zare, J. Chem. Phys. **72**, 6250 (1980).
20. A. Torres-Filho, J. G. Pruett, J. Chem. Phys. **72**, 6736 (1980).
21. A. M. F. Lau, Phys. Rev. A **13**, 139 (1976) and **19**, 1117 (1979); J. M. Yuan, T. F. George, F. J. McLafferty, Chem. Phys. Lett. **40**, 163 (1976); J. M. Yuan, T. F. George, J. Chem. Phys. **70**, 990 (1979); A. E. Orel, W. H. Miller, J. Chem. Phys. **70**, 4393 (1979) and **73**, 241 (1980).
22. P. Hering, P. R. Brooks, R. F. Curl Jr, R. S. Judson, R. S. Lowe, Phys. Rev. Lett. **44**, 687 (1980). □